Journal of the Ceramic Society of Japan, Supplement 112-1, PacRim5 Special Issue, 112 [5] S1084-S1088 (2004)

Paper

Elasticity and Thermal Conductivity of Porous Ceramics with Controlled Pore Structure

Jang-Hoon HA, Jong Ho KIM and Do Kyung KIM

Department of Materials Science and Engineering, Korea Advanced Institute of Science and Technology, 373-1, Kusong-dong, Yusong-gu, Taejon 305-701, Korea

The mechanical and thermal properties of porous ceramics with the controlled pore design were investigated through experiments and numerical analysis. Porous alumina ceramics containing well-defined pore shape, size and distribution were prepared by incorporation of fugitive additives into alumina. Processing variables provide various microstructure and the amount of porosity as well. Young's modulus and thermal conductivity were evaluated by resonant frequency and laser flash method, respectively. Elasticity changes with different pore structure were calculated by using finite element analysis (FEA) and compared with experimental data. Finite element analysis was confirmed as a useful tool to simulate the effect of pore structure on the mechanical and thermal properties of porous ceramics. The design parameter of pore structure of porous ceramics will be discussed based on the result of analysis. [Received August 8, 2003; Accepted December 24, 2003]

Key-words : *Elastic modulus, Thermal conductivity, Porous, FEM*

1. Introduction

Naturally occurring materials are often porous, some others are porous due to the result of processing. When materials contain pores or flaws, they influence the elastic and mechanical properties. In general, ceramic materials have good properties such as high wear resistance, hardness, thermal shock resistance and corrosion resistance. The presence of small pores results in a sharp decrease in strength and elastic modulus. Hence, the study on the effect of the microstructure on the macroscopic properties is important. The rule of mixture cannot explain the drastic change of properties, because it doesn't include the microscopic geometry.

Pore structure fabrication is important for both investigation and application and there are various ways to fabricate pore structures, such as, incomplete sintering of dense, porous particles or mixtures of these with various degrees of packing, addition of fugitive material to be removed in the early stages of sintering, forming operations such as extrusion, injection molding, and rapid prototyping methods that form pores and so on.[1] In this work, isolated pore structure was made by fugitive material removal method, and interconnected pore structure was made by incomplete sintering method.

There are two approaches for the elastic modulus-porosity correlation of ceramic materials. One is analytic predictions, which have a theoretical background on analytic solution of elasticity. So, its application is strongly limited on preliminary suggested solution. Much research has been done to find a property-porosity relationship when pore shape is regular like spherical, ellipsoidal, and crack.[2)-5)] The other is numerical simulation, which can represent any kind of shapes. If numerical simulation has a validity confirmation on elastic modulus calculation, then it can be used to predict elastic properties as a powerful tool. Finite element analysis is a universal tool and any desired shape and structure can be easily analyzed.

The aim of this study is to obtain the desired properties by controlling the pore shape and structure. Elastic modulus is a fundamental property of structural materials, moreover, in ceramic materials low Young's modulus is a barrier of structural application with low strength. The porous materials have to keep structural reliability for practical use, so the pore shape, structure, size and orientation must be controlled. To show the guideline for good mechanical characteristics, the morphology-elasticity relationship has to be presented. Random pore morphology may be more close to real pore morphology[6),7)] and the focus of the previously mentioned case is not a profitable pore model suggestion. Considering periodic pore shape and structure is fit to the aim and isolated pore structure and interconnected pore structure were modeled. These two kinds of model structure had periodical pores which could be represented by experiment with model material.

This paper reports on a study of thermal conductivity, because thermal insulation is a major application of porous materials. Three-dimensional model pore structures which were made for elastic properties simulation could be converted for thermal properties simulation with ease and prepared specimens could also be measured for the two kinds of properties.

2. Experimental

2.1 Three dimensional FEM modeling

In the present study, the Finite Element Method (FEM) has been used to compute the influence of porosity on elastic modulus. Two-dimensional (2D) FEM simulation is widely used because of its simplicity and versatility. It is obvious that 2D FEM results have insufficient physical meaning, but it gives a lower limit of the three-dimensional (3D) elastic modulus. A cross section image of a specimen shows only a 2D image of the 3D pore shape, and it's not easy to reconstruct the 3D pore shape and pore structure from the 2D image.

Figure 1 shows the (111) plane cross-section of isolated pore structure and 3D unit cell, and **Fig. 2** shows the (111) plane cross-section of the inter-connected one. Clearly, the two pore structures have different spacing between pores and pore shapes, but the cross section is quite similar. Therefore, 2D analysis result can be ambiguous. Surely, the cross sections of the other planes like (100) or (110) plane may show distinct features. It contains a trap that produces an intended output, i.e., output can be dependent not only on pore structure, but also on user-choice. 3D analysis is a more fundamental approach to elastic modulus-porosity relationship.

COSMOS/Works was used as FEM simulation tool which was an extended module of 3D CAD program 'SolidWorks', The boundary condition of elastic property calculation was

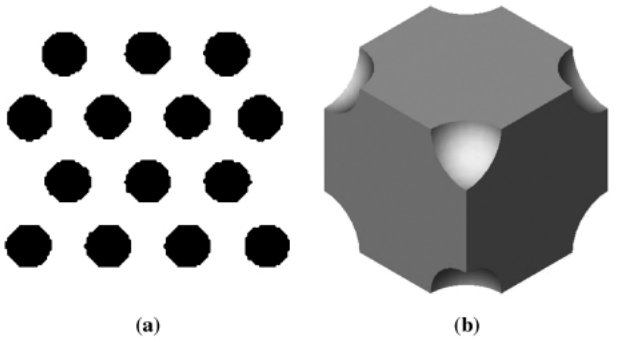

Fig. 1. Numerical analysis data of isolated pore structure (a) (111) cross section, (b) 3D unit cell.

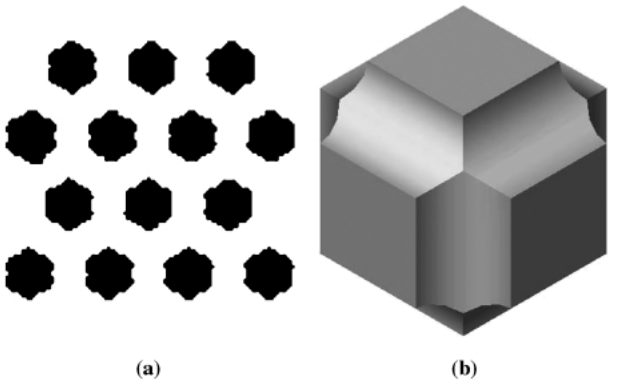

Fig. 2. Numerical analysis data of inter-connected pore structure (a) (111) cross section, (b) 3D unit cell.

very simple, so the model was loaded in tension by uniformly pressing normal to upper boundary plane and a point was fixed to restrain rigid body motion. The boundary conditions for thermal property calculation were similar to the ones for the elastic property calculation. Thermal flux was fixed, then temperature difference between upper and lower boundary plane was calculated. If the target model structure was random pore structure, very complex modeling would be required. Investigating periodic pore morphology had two main advantages. Firstly, it could be free from complex modeling or digital image acquisition and secondly it would be able to give a guideline to control pore structure. Computational simulation of pore interaction has to address the physical complexity of the pore microstructure and it has to satisfy practical computational consideration concerning model size. It is possible to concentrate computational ability to detailed mesh structure. The pore structures analyzed were made from three-dimensional, repetitive unit cells and only a small part of the structure needed to be analyzed.

With the same porosity, different pore structure induces different characteristics. Two common pore structures are isolated pore structure and interconnected pore structure. **Figure 3** shows the 3D FEM model of isolated pore structure and inter-connected pore structure. Isolated pore model structure was made of bulk material with spherical pores at grain junction. Inter-connected pore model structure was built of spherical particles. For comparison of spherical pores with ellipsoidal pores, aspect ratio of ellipsoidal pore was changed from 1 to 4.

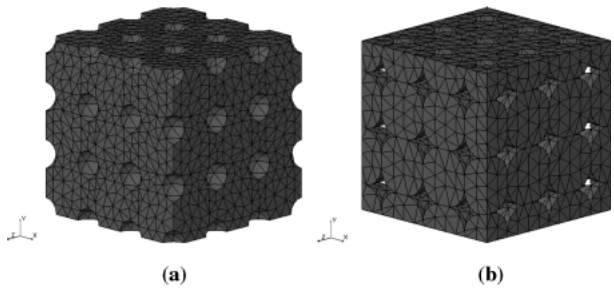

Fig. 3. 3D FEM model of (a) Isolated pore structure, (b) Interconnected pore structure.

2.2 Specimen preparation

Two kinds of model structure were fabricated. One was isolated pore structure and the other model pore structure was inter-connected pore structure.

2.2.1 Isolated pore structure

Starting powders were prepared comprising a mixture of AKP–50 (Sumitomo, Japan) and 8 μm Polymethyl methacrylate, PMMA (Aldrich, USA) in double distilled water. The slurries were ball-milled without milling balls for 5 h and then oven-dried at 60°C for 24 h. Green bodies were prepared by cold-isostatic pressing (CIP) and then sintered at 1600°C for 5 h using box furnace in air atmosphere. Processing method was 'Removal of fugitive material added to the body', In this study, the body and fugitive material were alumina and PMMA, respectively. Although the commercial PMMA powder had some size distribution, it had quite good sphere shape. To avoid PMMA shape deformation, organic solvent and mixing media were not used in the mixing process. Preliminary experiments showed that organic solvent caused PMMA dissolution and mixing media made PMMA sphere irregular shape. In sintering process, PMMA decomposition occurred around 450°C. When PMMA burned out, heating rate was 50°C/hr. It prevented evaporated PMMA gas from remaining in matrix. Well-defined spherical pores were formed in alumina matrix.

2.2.2 Inter-connected pore structure

Changing sintering temperature made it possible to form inter-connected pore structure. AKP–50 (Sumitomo, Japan) was used as the starting powder with no additives. When sintering temperature was low, densification and grain-growth were suppressed. Only necks were formed between particles. The pore structure of sintered body was inter-connected. Holding temperatures were 1100°C, 1200°C, 1300°C, 1400°C and 1500°C. When the porosity of specimen was low, the connectivity between pores was low. It had isolated pore structure characteristics irrespective of target pore structure being isolated or inter-connected. Similarly, when porosity was high, the overlap of pores could not be ignored. For pore structure identification, fracture surfaces of specimen were observed with SEM. Density was measured by Archimedes method.

2.3 Elastic modulus and thermal conductivity measurement

Elastic modulus measurement technique was impulse excitation of vibration method (ASTM E1876–1 Standard Test Method For Dynamic Young's Modulus, Shear Modulus and Poisson's Ratio by impulse excitation of vibration).

In general, well-known pulse-echo method was widely used. For highly porous materials, pulse-echo method was not adequate. Due to strong attenuation caused by scattering, (high frequency) ultrasonic pulse-propagation methods often cannot be used on small-sized specimens of porous materials.

Elastic modulus can be calculated directly using Eq. (1).

$$E = 0.9465 (m f_f^2 / b) (L^3 / t^3) T_1 \quad (1)$$

Where E = Young's modulus, (Pa), m = mass of the bar, (g), b = width of the bar, (mm), L = length of the bar, (mm), t = thickness of the bar, (mm), f_f = fundamental resonant frequency of bar in flexure, (Hz), and T_1 = correction factor for fundamental flexural mode to account for finite thickness of bar and Poisson's ratio, etc.

The resonant frequencies were measured using non-contact transducer (Cirrus ZE:901 CRL L3M Preamplifier). For measurement, prismatic shaped specimens (length 30–32 mm, width 5–6 mm, thickness 2–3 mm) were used.

Thermal conductivity was measured by hot disk method. A heat pulse was generated for a given time by passage of an electrical current through a very thin metallic foil combined heater/temperature sensor probe unit insulated on both surfaces and embedded between two pieces of the test specimen. The resulting temperature response was then analyzed in accordance with an appropriate model. For measurement, disk specimens (diameter 20 mm, thickness 2–5 mm) were used.

3. Results

3.1 Microstructure and porosity

Figure 4(a) shows fracture surface image of alumina with isolated pore structure (5% porosity). It was observed that spherical pores had the same size as that of PMMA particles in alumina matrix. Distinct spherical pores, which were not present in conventional sintering process could be seen. Well-defined isolated spherical pores were fabricated from 0% to 30% porosity. Fig. 4(b) shows fracture surface image of alumina with inter-connected pore structure (5% porosity). Comparing with isolated case, particles were connected with minimum solid contact. Interconnected pore structure could be fabricated from 0% to 45% porosity. Especially at high porosity, it showed well-interconnected pore structure.

3.2 Elastic modulus

Analytic calculation with several variables was done previously. FEM result and analytic calculation show similar trends.

$$E = E_0 \exp(-bp) \quad (2)$$

The general form of elastic modulus-porosity correlation is presented as a simple empirical Eq.[8] (2). E_0 is zero-porosity elastic modulus, P is the volume fraction of porosity and b is an empirical constant. Spriggs[9] showed that the constant b was 2.73 for slip casting and sintering; 4.08～4.35 for hot pressing; 3.44～3.55 for cold pressing and sintering.

Hasselman[10] proposed a general equation (3) of different form based on solutions of the elastic moduli of heterogeneous system. This expression suggested a continuous phase containing a dispersed phase of spherical pore.

$$E = E_0 \left[1 + \frac{AP}{1 - (A+1)P} \right] \quad (3)$$

where E = elastic modulus (shear or bulk) of composite, E_0 = elastic modulus of continuous phase.

E_0 and A are to be determined statistically from experimental data. Hasselman's equation was valid for only spherical pores. In this study, modified Hasselman's equation could be derived by FEM simulation. The simple constant A could be replaced

$$A = -2\left(\frac{a}{c}\right) \quad \text{when} \quad \left(\frac{a}{c}\right) \geq 1 \quad (4)$$

$$A = -1 - \left(\frac{a}{c}\right) \quad \text{when} \quad \left(\frac{a}{c}\right) < 1 \quad (5)$$

It was suggested that Hasselman's equation could be extended to ellipsoidal pore with the aid of numerical calculation.

The dependence of pore structure on the elastic modulus is shown in **Fig. 5**. Elastic modulus of interconnected pore structure was more sensitive to porosity than isolated one. When loading direction was parallel to major axis of ellipse, it was predicted that elastic modulus was not changed much and elastic modulus was less dependent on porosity. On the other hand, when loading direction was normal to major axis of ellipse, elastic modulus significantly changed with increasing porosity. In **Fig. 6**(a), and (b) black line shows a trend that aspect ratio of ellipse was one (i.e., spherical pore). At the

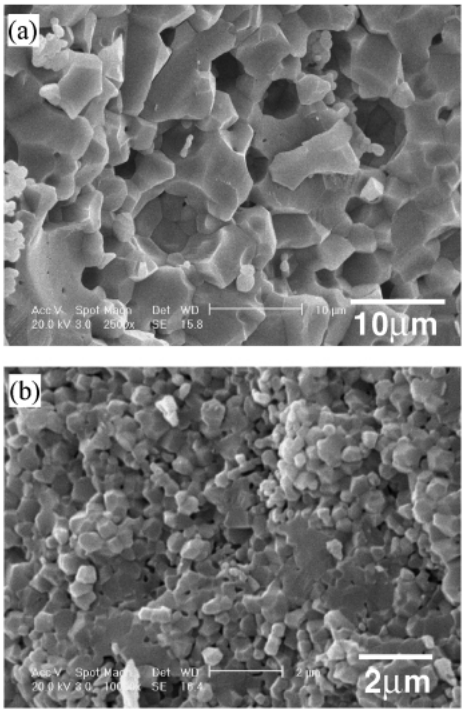

Fig. 4. Fracture surface image of alumina with 5% porosity (a) Isolate pore structure, (b) Inter-connected pore structure.

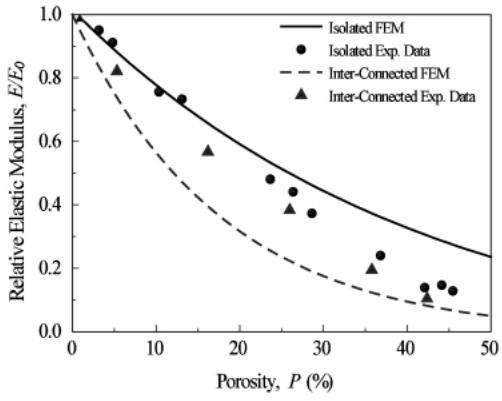

Fig. 5. Comparison of relative elastic modulus of FEM simulation result with experimental data having different pore structure.

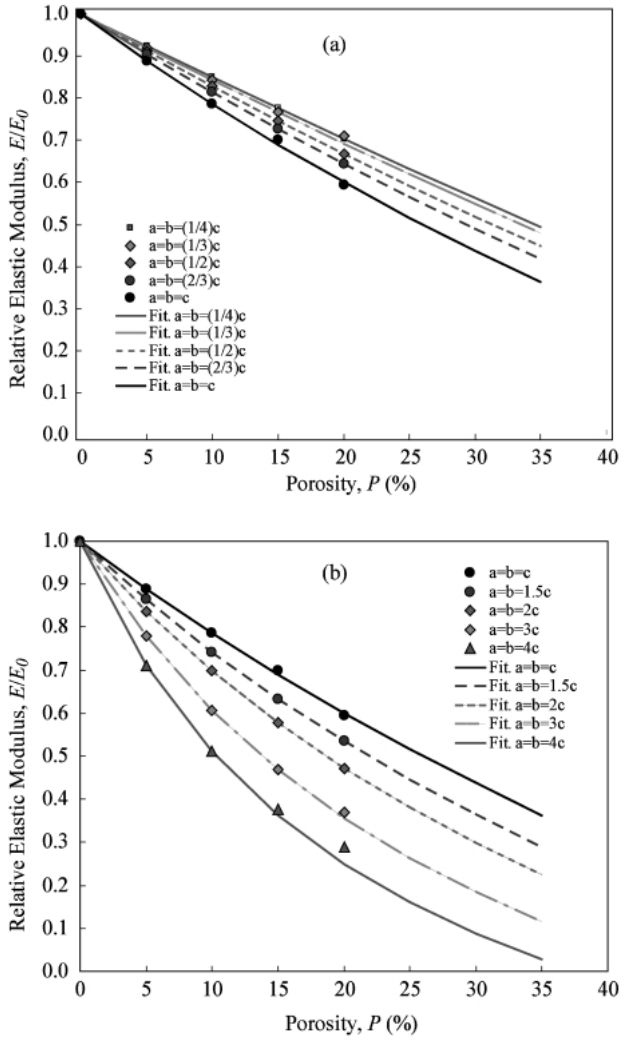

Fig. 6. Elastic modulus change when loading direction is (a) parallel with major axis of ellipse, (b) normal to major axis of ellipse.

same porosity, as aspect ratio decreased, elastic modulus increased. When loading axis was normal to major axis of ellipse, thermal conductivity decreased with the increase in aspect ratio.

3.3 Thermal conductivity

Thermal property shows similar trends with elastic property. Same pore model and same analytic equation could be used and the dependence of pore structure on the thermal conductivity is shown **Fig. 7**. In FEM trends, interconnected pore structure was more sensitive to porosity on elastic modulus than isolated one. Experimental data line shows thermal conductivity data of isolated pore structure specimen. In **Fig. 8** (a), (b) black line shows trend that aspect ratio of ellipse is one (i.e., spherical pore). At the same porosity, as aspect ratio decreased, thermal conductivity increased when thermal flux axis was normal to major axis of ellipse. As aspect ratio increased, thermal conductivity decreased.

4. Discussions

Isolated pore structure and interconnected pore structure were fabricated with wide range of porosity. PMMA particles could be used to induce spherical pores. It was more profitable to compare FEM result with spherical pore than irregular pore, induced by corn starch or potato starch. Inter-connected

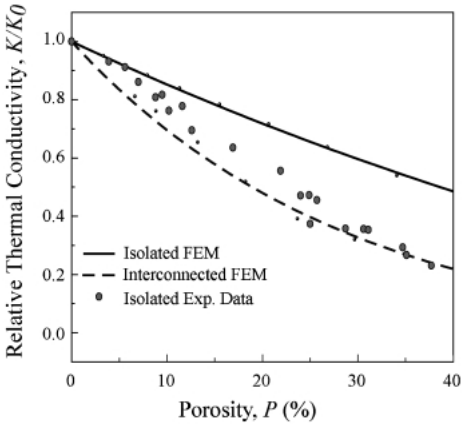

Fig. 7. Comparison of relative thermal conductivity of FEM simulation result with experimental data having different pore structure.

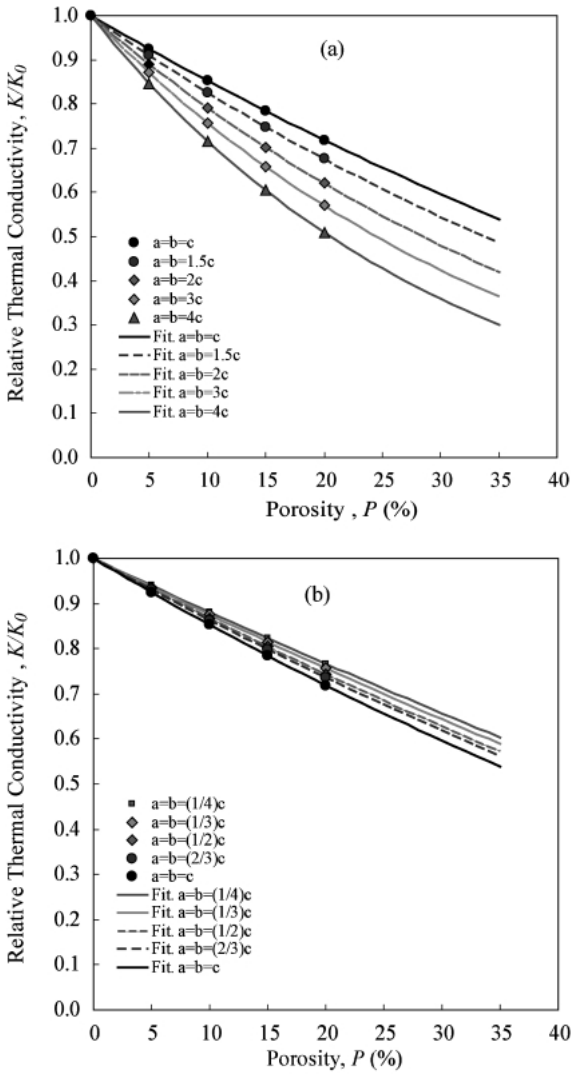

Fig. 8. Thermal conductivity change when loading direction is (a) parallel with major axis of ellipse, (b) normal to major axis of ellipse.

pore structure also showed quite well defined pore structure. Only necks were formed between particles. It made it possible to confirm FEM result of minimum solid area model.

Development of analysis tools to evaluate mechanical and thermal properties of porous ceramic materials has been achieved. One useful approach for mechanical and thermal properties estimation is finite element method (FEM). The three dimensional FEM is useful to simulate pore structure and pore shape. Both elastic modulus and thermal conductivity can be predicted successfully by FEM.

In empirical equation, despite quite good approximation, if the pore shape and structure is changed, the determination of empirical constant b was not well understood. It is the best fit to experimental data and it's not based on theory but entirely empirical, and cannot be regarded as entirely valid. Therefore, necessity of modified equation is emphasized.

To confirm the validity of the FEM results, comparison of the FEM results and experimental data was needed. Comparison of spherical pore FEM result with experimental data shows quite good agreement. It is possible to predict the properties of ellipsoidal pore using FEM result. Elastic modulus and thermal conductivity of interconnected pore structure was more sensitive to porosity than isolated one. It was due to its minimum contact area between particles. At low porosity, isolated spherical pores and high porosity inter-connected pores were made successfully. Regardless of target pore structure, when porosity went higher it had mixedup structure and inter-connected pore. As porosity reached about 40%, it lost characteristics of isolated pore structure. Overlap of pores made the connectivity of pores higher, and imperfect sintering was caused due to high percentage of fugitive material. Observation from microstructure predicted that the elastic modulus value would be lower than FEM result. In contrast to isolated pore structure, as specimen was more porous, its characteristics of interconnected pore structure could be found easily. At low porosity the inter pore distance got longer, then it lost its connectivity and its own characteristics.

As aspect ratio of ellipsoidal pore changes, elastic modulus and thermal conductivity show different trends. It was thought that stress concentration and thermal flux disturbance caused these results. To maximize the advantage of porous material properties, high aspect ratio pores have to be considered. Due to relatively limited experimental data, well-defined model pore structure is required to show validity of analysis.

5. Conclusions

The three dimensional FEM is useful to simulate pore structure and pore shape. Elastic properties and thermal properties show similar dependence on pore structure and pore shape. In a point of view with pore structure, inter-connected pore structure is more sensitive to porosity than isolated pore structure. As aspect ratio of ellipsoidal pore becomes higher, it is predicted that elastic modulus and thermal conductivity are more sensitive to porosity, if loading is normal to major axis of ellipsoidal pore. The optimum design parameter of pore structure and pore shape in porous ceramics has been discussed based on the result of analysis.

Acknowledgment This work is supported by Center for Advanced Materials Processing (CAMP) of the 21st Century Frontier R&D program funded by Korean Ministry of Science and Technology.

References

1) Rice, R. W., "Porosity of Ceramics," Marcel Dekker, Inc., New York (1997) pp. 20–21.
2) Hashin, Z., *J. Appl. Mater.*, Vol. 50, pp. 481–505 (1983).
3) Luo, J. and Stevens, R., *J. Appl. Phys.*, Vol. 79, pp. 9047–9056 (1996).
4) Rice, R. W., *J. Mater. Sci.*, Vol. 31, pp. 102–118 (1996).
5) Tsukrov, I. and Novak, J., *International Journal of Solids and Structure*, Vol. 39, pp. 1539–1555 (2002).
6) Roberts, A. P. and Garboczi, E. J., *Acta Mater.*, pp. 189–197 (2001).
7) Roberts, A. P. and Garboczi, E. J., *J. Mech. Phys. Solids*, Vol. 50, pp. 33–55 (2002).
8) Knudsen, F. P., *J. Am. Ceram. Soc.*, Vol. 45, pp. 94–95 (1962).
9) Spriggs, R. M., *J. Am. Ceram. Soc.*, Vol. 45, pp. 454 (1962).
10) Hasselman, D. P. H., *J. Am. Ceram. Soc.*, Vol. 45, pp. 452–453 (1962).